Microchimica Acta
https://doi.org/10.1007/s00604-018-2972-6

ORIGINAL PAPER

Voltammetric immunoassay for *Mycobacterium tuberculosis* secretory protein MPT64 based on a synergistic amplification strategy using rolling circle amplification and a gold electrode modified with graphene oxide, Fe_3O_4 and Pt nanoparticles

Dan Gou[1] · Guoming Xie[2] · Yuxia Li[1] · Xin Zhang[1] · Hui Chen[1]

Received: 13 May 2018 / Accepted: 23 August 2018

Abstract

The authors describe an electrochemical immunoassay for ultrasensitive determination of the *Mycobacterium tuberculosis (MTb)* secretory protein MPT64 which is an antigen for early diagnosis of infection with *MTb*. Protein G was used to immobilize antibodies against MPT64 on a gold electrode. Graphene oxide with its large surface area was used as a carrier to anchor magnetite (Fe_3O_4) and platinum (Pt) nanoparticles. The nanocomposite of type GO@Fe_3O_4@Pt was used as a signal reporter with excellent catalytic activity and recyclability. The nanocomposite exhibits peroxidase-like activity for hydrogen peroxide, best at −0.25 V (vs. Ag/AgCl). It works over a wide range of pH values (2–10) and temperatures (25–65 °C). Further signal amplification strategy was accomplished by rolling circle amplification. This voltammetric assay has a linear response to the logarithm of MPT64 concentration in the range from 5.0 fg·mL^{-1} to 1.0 ng·mL^{-1} and a detection limit of 0.34 fg·mL^{-1} (at a signal to noise ratio of 3, for $n = 10$). The assay can be completed within 4 h. It was successfully applied to the determination of MPT64 in spiked serum samples. Conceivably, the assay has a large potential in providing laboratory evidence for rapid diagnosis of *MTb* infection.

Keywords MPT64 · Aptamer primer · Biosensor · Nanocomposite · Magnetite · Protein G · Horseradish peroxidase · Differential pulse voltammetry · Circular DNA

Introduction

Tuberculosis (TB), a critical disease caused by *MTb*, remains a global health issue [1]. In 2016, it was estimated that approximately 10.4 million people developed TB, but only 6.3 million new cases were diagnosed and reported officially. And an estimated 1.7 million people died of TB with most deaths ascribed to the large gaps in proper diagnosis and follow-up treatment [2]. Hence, it is urgent to develop an appropriate method to detect *MTb* for early and rapid diagnosis of TB.

At present, the detection methods for *MTb* mainly include bacterial culture [3], sputum smear microscopy [4], tuberculin skin test and fluorescence quantitative PCR [5]. Bacterial culture is still the gold standard for *MTb* detection. However, this method cannot be widely used because it is time-consuming (4–6 weeks). Although sputum smear microscopy is widely used because it is simple and cost-effective, the sensitivity needs to be improved. The tuberculin skin test is not suitable for people who are immunocompromised or those who have been vaccinated with *Bacillus Calmette-Guerin* [6]. Although fluorescence quantitative PCR has high sensitivity and accuracy for detection of *MTb*, a professional trained staff is needed to operate the rigorous experimental protocol, which limits its application in primary medical units. Yin et al. reported that *MTb* secretory protein MPT64 was a specific antigen for the

Electronic supplementary material The online version of this article (https://doi.org/10.1007/s00604-018-2972-6) contains supplementary material, which is available to authorized users.

✉ Hui Chen
huichen@hospital.cqmu.edu.cn

[1] Clinical Laboratories, The First Affiliated Hospital of Chongqing Medical University, No. 1, You Yi Road, Yu Zhong District, Chongqing 400016, People's Republic of China

[2] Key Laboratory of Laboratory Medical Diagnostics, Ministry of Education, Department of Laboratory Medicine, Chongqing Medical University, Chongqing 400016, People's Republic of China

Published online: 30 August 2018

early diagnosis of *MTb* infection [7] . Purohit et al. proposed an immunostaining method based on MPT64 for diagnosis of *MTb* infection [8]. A micro-fluidic biosensor was proposed to diagnose TB by the detection of MPT64, but the sensitivity required improvement [9]. Furthermore, a voltammetric biosensor was developed to quantitate MPT64, but the use of non-conductive chitosan reduces the sensitivity of the method [10]. Therefore, it is necessary to investigate a rapid and accurate method with desirable sensitivity and specificity for the early diagnosis of *MTb* infection by a good marker, such as MPT64.

To enhance the performance of the new method, a good way is to introduce nanocomposite. GO can strongly adsorb single-stranded DNA (ssDNA) through π stacking interactions [11]. This property determines that GO can be used in conjunction with a nucleic acid amplification system such as rolling circle amplification (RCA). For the large surface area, GO is also a good carrier to anchor nanoparticles. Both Fe_3O_4 and Pt nanoparticles have catalytic activity, especially the Pt nanoparticles [12]. However, the widespread use of Pt nanoparticles is not feasible for its rare and expensive. Thus, we try to synthesize GO@Fe_3O_4@Pt nanocomposite. It can both adsorb ssDNA and has excellent catalytic activity, and can also be reused easily by magnetic separation.

RCA, an isothermal amplification platform, has received increasing attention due to its simplicity and high efficiency [13]. Compared with other isothermal amplification platforms, such as hybridization chain reaction [14] and loop-mediated isothermal amplification [15], RCA does not require a complicated design of hairpin probes or primers. In a typical RCA process, a short DNA primer is first hybridized to the circular DNA template (cDNA), and then the primer is extended continuously around the cDNA with the help of phi29 DNA polymerase. Finally, extremely long ssDNA is obtained, which contains thousands of tandem repeats.

As the aptamers, single-stranded oligonucleotides (DNA or RNA) have the advantages of flexible modification, low cost, high affinity and specificity toward target [16]. In previous research, our group described a biosensor to detect Staphylococcal enterotoxin B with the recognition element of DNA aptamer [17]. A new electrochemical method is presented here for ultrasensitive detection of *MTb* secretory protein MPT64. A GO@Fe_3O_4@Pt nanocomposite was synthesized and used as a signal reporter by efficiently catalysing the decomposition of H_2O_2. APP was used to both specifically recognize MPT64 and trigger the amplification process of RCA reaction. Because RCA products (RCPs) are long ssDNA, they can be strongly adsorbed by GO@Fe_3O_4@Pt nanocomposite to greatly amplify the detection signal. This synergistic amplification strategy based on GO@Fe_3O_4@Pt nanocomposite and rolling circle amplification has not been reported previously. Because protein G (PG) can force the antibody to expose its binding sites by specifically interacting with antibody's fragment crystallizable region [18], it was used to immobilize antibodies on electrode surface. This contributed to improve the efficiency of capturing MPT64. The stepwise fabrication process and assay principle are depicted in Scheme 1. As expected, with the increasing concentration of MPT64, the amplified current signal increased accordingly. Therefore, this electrochemical biosensor has great potential in clinical application for early and rapid detection of *MTb*.

Experimental

Reagents and materials

GO was purchased from Pioneer Nanotechnology Co. (Nanjing, China, http://www.xfnano.com). Amino-functionalized Fe_3O_4 nanoparticles (100–200 nm) were obtained from Aladdin (Shanghai, China, http://www.aladdin-e.com). Chloroplatinic acid hexahydrate ($H_2PtCl_6{\cdot}6H_2O$), 1-ethyl-3-3(3-dimethylaminopropyl) carbodiimide (EDC), N-hydroxysuccinimide (NHS), and bovine serum albumin (BSA, 96–99%) were purchased from Sigma-Aldrich (St. Louis, MO, USA, http://www.sigmaaldrich.com). All oligonucleotide sequences were synthesized and purified by high-performance liquid chromatography (HPLC) at Beijing Genomics Institute (BGI, China, http://www.genomics.cn). The sequences are listed in Table S1. The antibody against *MTb* secretory protein MPT64 (anti-MPT64) was obtained from Lifespan Biosciences, Inc. (Seattle, USA, https://www.lsbio.com). Recombinant MPT64 protein and *MTb* secretory protein Ag85B were obtained from CUSABIO (Wuhan, China, http://www.cusabio.cn). T4 DNA ligase, phi29 DNA polymerase, exonuclease I (Exo I) and exonuclease III (Exo III) were purchased from Thermo Fisher Scientific (MA, USA, https://www.thermofisher.com). *His-tagged* recombinant protein G, deoxyribonucleotide triphosphate mixture (dNTPs) and 3,3′,5,5′-tetramethylbenzidine (TMB) were purchased from Sangon Biotechnology, Co. (Shanghai, China, http://www.sangon.com). Ultrapure water (Milli-Q18.2 MΩ·cm, Millipore System, Inc.) was employed in all the experiments. All other reagents used in this work were of analytical grade without further purification.

Apparatus and measurements

Cyclic voltammetry (CV), electrochemical impedance spectroscopy (EIS) and differential pulse voltammetry (DPV) were carried out on a CHI 660E electrochemical

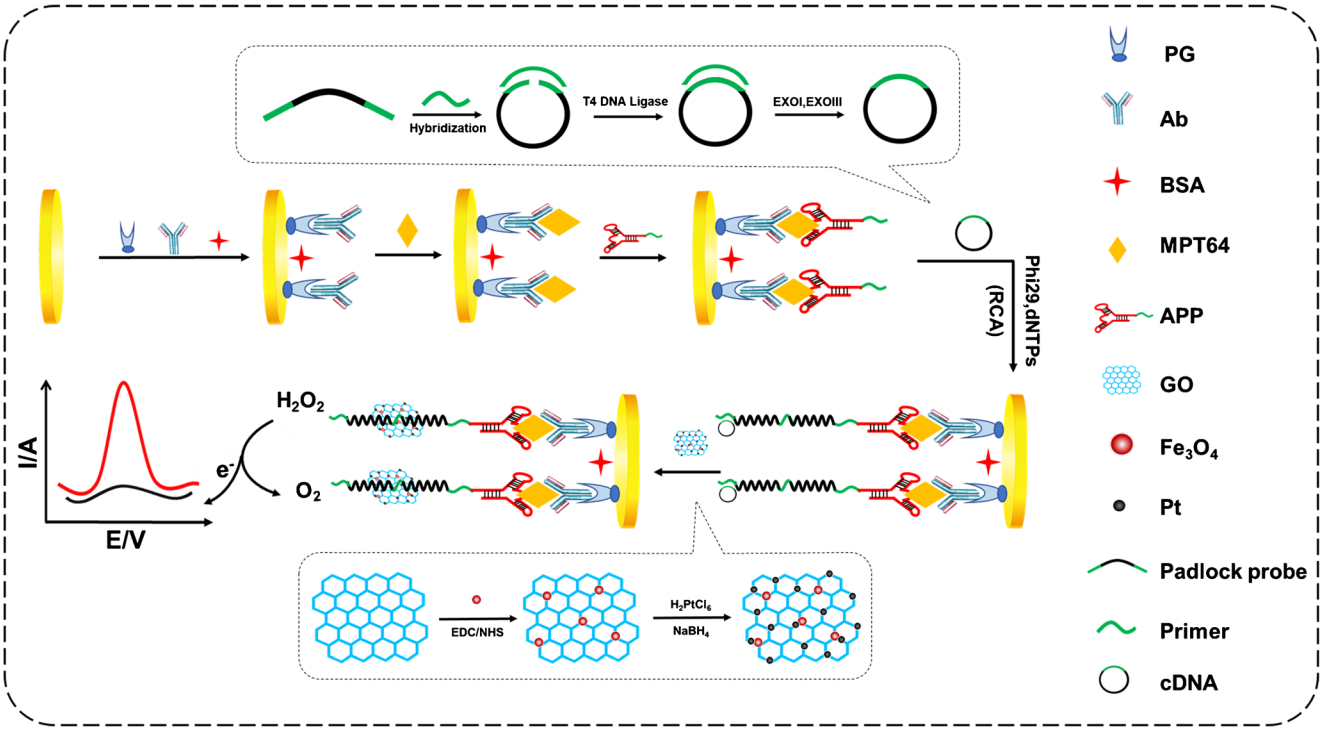

Scheme 1 Schematic of electrochemical detection of MPT64

workstation (Shanghai Chenhua Instruments Co., China). The EIS data was fitted with the equivalent circuit model by Zview 2 software. Gold electrode was used as a working electrode, Pt wire and Ag/AgCl (in saturated KCl) served as counter electrode and reference electrode, respectively. Transmission electron microscopy (TEM, JEM-1400 Plus, Japan) was used to characterize the morphology of nanomaterials. An energy dispersive spectrometer (EDS, Merlin Compact, Germany) was used to analyse the components of nanomaterial. The absorbance was recorded by Multi-Mode Microplate Reader (Biotek Eon, Vermont, USA). Fluorescence spectra were measured by a Cary Eclipse fluorescence spectrophotometer (Agilent, California). All measurements were performed at room temperature unless otherwise stated.

Preparation of GO@Fe_3O_4 nanocomposite

First, the solid GO was dissolved in ultrapure water with more than 2 h ultrasonication to form a homogeneous GO solution (1 mg·mL^{-1}). Then, the carboxylic group of GO was activated by 75 mmol·L^{-1} EDC and 25 mmol·L^{-1} NHS with stirring vigorously at room temperature for 1 h. The activated GO was collected by centrifugation at 8000 rpm (4310 rcf) for 10 min. Then, amino-functionalized Fe_3O_4 nanoparticles (1 mg·mL^{-1}) was added to the activated GO solution with stirring at 50 °C for 1 h. After magnetic separation, the GO@Fe_3O_4 nanocomposite was obtained and stored at 4 °C for further use.

Synthesis of GO@Fe_3O_4@Pt nanocomposite

GO@Fe_3O_4@Pt nanocomposite was synthesized by in-situ reduction of Pt ions according to the literature with modification [12]. Briefly, the prepared GO@Fe_3O_4 nanocomposite (1 mg) was added to chloroplatinic acid hexahydrate solution ($H_2PtCl_6{\cdot}6H_2O$, 1%, 2 mL). After mixing thoroughly, the mixture was kept in the shaking table at 30 °C for 12 h so that the $H_2PtCl_6{\cdot}6H_2O$ was adsorbed onto GO@Fe_3O_4 surface sufficiently. The free $H_2PtCl_6{\cdot}6H_2O$ was removed by magnetic separation. Subsequently, the solid was transferred to a glass bottle with 2 mL of ultrapure water. Sodium borohydride ($NaBH_4$, 1%) was added to reduce Pt ions in-situ with ultrasonication for 30 min. Finally, the GO@Fe_3O_4@Pt nanocomposite was obtained by magnetic separation and stored at 4 °C for future use.

Preparation of the circular DNA template

The primer (0.5 μmol·L^{-1}) and phosphorylated padlock probe (0.5 μmol·L^{-1}) containing two complementary sequence regions with primer were hybridized by heating at 95 °C for 5 min and cooling down to 22 °C gradually over 1 h (almost 1 °C/min) to form circular DNA. T4 DNA ligase (0.5 U/μL) was used to connect the nick in the cDNA at 22 °C overnight in a 20 μL reaction system. The product was obtained by ethanol precipitation after deactivation of T4 DNA ligase at 65 °C for 15 min. The leftover ssDNA or dsDNA were digested by Exo I (2 U/μL) and Exo III (5 U/μL). After the enzymes denatured at 85 °C for 15 min, the cDNA was

purified by ethanol precipitation again. The concentration of cDNA was measured by NanoDrop.

Fabrication of the biosensor

The gold electrode (3 mm diameter) was polished with alumina slurry (0.3 μm and 0.05 μm) on a polishing cloth, followed by ultrasonic cleaning of the electrode in ultrapure water, absolute ethyl alcohol and ultrapure water, respectively, for 10 min. After being treated with freshly prepared piranha solution (98% H_2SO_4:30% H_2O_2, 3:1 *v*/v), a mirror-like surface was obtained on gold electrode. The prepared electrode was incubated with *his-tagged* PG (15 μg·mL^{-1}) at 4 °C for 2 h. After washing with phosphate buffer (PB, 10 mmol·L^{-1}, pH 7.4), it was immersed in anti-MPT64 (20 μg·mL^{-1}) at 4 °C overnight. In order to reduce the non-specific adsorption, 0.25% BSA was applied to block the non-binding sites on the surface of the gold electrode at room temperature for 1 h. Finally, the biosensor was obtained after another round of washing with PB and stored at 4 °C by immersed in PB (10 mmol·L^{-1}, pH 7.4) for future use.

Determination of MPT64 protein by electrochemical biosensor

The prepared biosensor was incubated with 10 μL of different concentrations of MPT64 at 37 °C for 1 h. Tris-HCl buffer (20 mmol·L^{-1}, pH 8.0) was used to dilute MPT64. After washing with PB (10 mmol·L^{-1}, pH 7.4), 10 μL of 200 nmol·L^{-1} APP probe was dropped on the electrode and incubated at 37 °C for 1 h. Subsequently, the electrode was immersed in the RCA reaction solution to proceed at 37 °C for 1 h. The composition of the RCA reaction solution was cDNA (100 nmol·L^{-1}), dNTPs (0.5 mmol·L^{-1}), phi29 DNA polymerase (0.1 U/ μL) and 10 × RCA reaction buffer (33 mmol·L^{-1} Tris-HCl (pH 7.9), 10 mmol·L^{-1} $MgCl_2$, 66 mmol·L^{-1}KCl, 0.1% (*v*/v) Tween 20, 1.0 mmol·L^{-1} dithiothreitol). Then, the reaction solution on the electrode surface was washed out thoroughly. Afterward, the GO@Fe_3O_4@Pt nanocomposite (10 μL, 0.5 mg·mL^{-1}) was dropped on the electrode and incubated at 37 °C for 40 min. Then, the electrode was immersed in PB working solution (10 mmol·L^{-1}, pH 4.0) containing 20 mmol·L^{-1} H_2O_2 for DPV measurement (from −0.6 V to 0.1 V at the sweep rate of 50 mV s^{-1}). The measurement process of MPT64 in unknown (real) samples was the same as the above steps and the concentration can be calculated by calibration plot.

Results and discussion

Choice of materials

GO was graphene-family nanomaterial with a large surface area. It has attracted widespread attention due to its excellent physicochemical properties [19]. For example, Chen et al. utilized the large surface area of the reduced GO to load polyaniline for the detection of *MTb* [20]. Li et al. built a biosensor for microRNA detection based on GO's strong adsorption with single-stranded DNA [21]. These researches indicated that GO was a good candidate both in loading materials and in interacting with DNA. Magnetic nanomaterials were used in many fields for separation, such as water purification, food production and medical science [22]. Interestingly, Fe_3O_4 nanoparticles not only possess magnetic property, but also have catalytic activity [23]. Pt is a noble metal nanomaterial best known for its excellent catalytic activity, such as carbon monoxide oxidation, methanol oxidation, and hydrogen oxidation [24]. However, the widespread use of Pt is limited because it is rare and expensive. Thus, it is necessary to recycle Pt to reduce the cost of corresponding methods. In the comprehensive consideration of the properties of GO, Fe_3O_4, and Pt, GO@Fe_3O_4@Pt nanocomposite was synthesized. Combined the catalytic activity of Fe_3O_4 and Pt for the decomposition of H_2O_2, a much higher electron transfer signal was detected. Importantly, the nanocomposite can be reused by magnetic separation.

Characterization of the GO@Fe_3O_4 and GO@Fe_3O_4@Pt

The morphology of GO@Fe_3O_4 and GO@Fe_3O_4@Pt were characterized by TEM. Figure 1a shows that Fe_3O_4 nanoparticles are anchored on the GO surface. This indicates that GO@Fe_3O_4 is synthesized successfully via covalent bonding of carboxyl groups to amino groups. After the in-situ reduction of Pt ions, large amounts of small Pt nanoparticles are uniformly distributed on the surface of GO@Fe_3O_4 nanocomposite (Fig. 1b). The EDS technique was used to confirm the presence and distribution of the elements of GO@Fe_3O_4@Pt. As shown in Fig. 1c, the peaks of Fe, Pt, C, and O are clearly observed, which indicates that Fe_3O_4 and Pt nanoparticles are well anchored on the GO surface.

To verify the catalytic activity of GO@Fe_3O_4@Pt nanocomposite, both GO@Fe_3O_4@Pt and HRP were treated at a range of pH (2.0–10.0) and temperatures (25–65 °C) for 30 min, respectively. The results indicate that GO@Fe_3O_4@Pt nanocomposite can endure the harsh conditions in comparison with HRP (Fig. S1). Moreover, the recyclability of the GO@Fe_3O_4@Pt nanocomposite was also investigated (Fig. S2). The interaction of GO@Fe_3O_4@Pt nanocomposite with ssDNA was analysed by a fluorescent probe. The results demonstrate that GO@Fe_3O_4@Pt nanocomposite can adsorb ssDNA as well as GO. It can be a good signal reporter through the adsorption with ssDNA produced by RCA (Fig. S3).

Validation of rolling circle amplification

Agarose gel electrophoresis assay (120 V, 30 min) was used to validate that cDNA was synthesized successfully and RCA

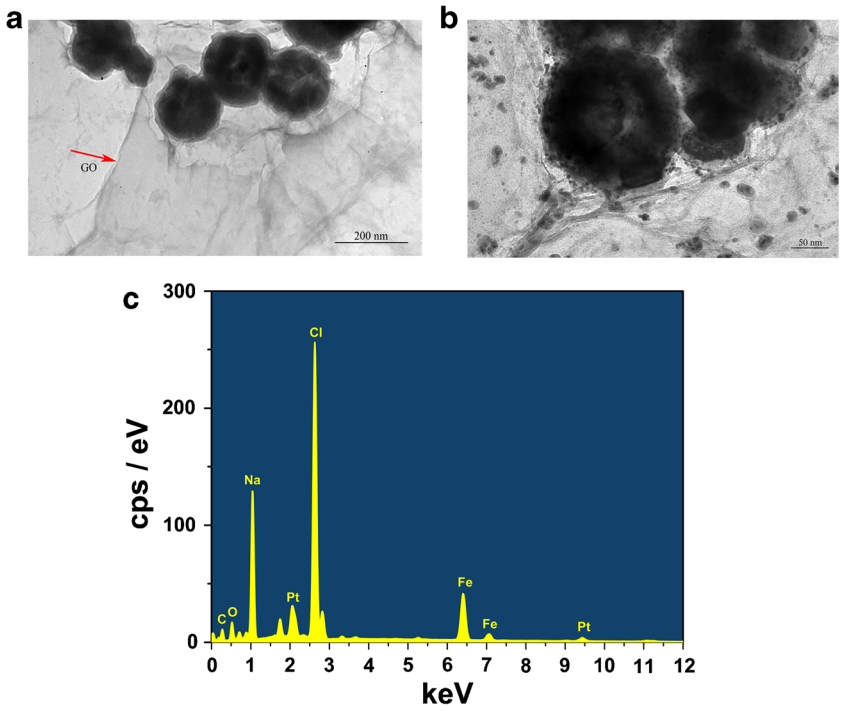

Fig. 1 Characterization of nanocomposite. **a** TEM image of GO@Fe_3O_4. **b** TEM image of GO@Fe_3O_4@Pt. **c** EDS pattern of GO@Fe_3O_4@Pt

can be performed well. As shown in Fig. S4a, there is one bright black band and many sub-bands in lane 3 after T4 DNA ligase incubation with padlock probe and primer. The bright black band is considered as cDNA for its position in the lane, which is supported by Roh's report [25]. The sub-bands are the excessive padlock probe and primer or the mismatch between them. After being treated with Exo I and Exo III, the sub-bands in mixture are disappeared, leaving the cDNA only (lane 4). This suggests that cDNA is prepared successfully for its resistance to enzymatic digestion. Whether the APP probe can trigger RCA reaction like a primer was also examined. As seen in Fig. S4b, large molecule weight RCPs are observed in both lane 3 and lane 4 using primer and APP, respectively, for RCA reaction. These RCPs are the bright black bands which barely move in gel analysis. In contrast, RCPs cannot be observed in lane 1 and lane 2 due to the lack of cDNA in RCA reaction solution. These results indicate that APP can be served as a primer to trigger RCA reaction, and cDNA is successfully synthesized in this work. Figure S5 further indicates that RCA signal amplification strategy coupled with GO@Fe_3O_4@Pt nanocomposite can effectively improve the sensitivity.

Electrochemical characterization of the modified electrode

The stepwise modification processes of the gold electrode were characterized by CV in PB working solution (10 mmol·L^{-1}, pH 7.4) containing 5 mmol·L^{-1} $K_3[Fe(CN)_6]$/$K_4[Fe(CN)_6]$ and 0.1 mol·L^{-1} KCl at a scan rate of 0.1 V/S. As described in Fig. 2a, the current response of the modified electrode is decreased evidently due to the electron transfer being hindered by nonconductive substances (including PG, anti-MPT64, BSA, APP and RCPs). Compared with bare gold electrode (curve a), PG modified electrode has a reduced current response value (curve b), which demonstrates that PG is connected successfully on the surface of gold electrode due to the well-known affinity of *his-tag* to gold [26]. After anti-MPT64 and BSA are fixed on the electrode, the current response is decreased further (curve c and curve d). With the MPT64 being captured as a target, the current response is decreased again (curve e). Curve f and curve g represent the results of APP fixed and subsequent RCA reaction on the gold electrode. This suggests that APP is connected successfully on the electrode surface by specific recognition of MPT64, and then trigger RCA reaction after the gold electrode immersed in RCA reaction solution. The CV results were further verified by EIS (high frequency: 10^5 Hz, low frequency: 0.1 Hz) which suggested that the constructed biosensor is feasible (see electronic supplementary material 1.6 for details).

Optimization of experimental conditions

Various experimental parameters were optimized, including the different APP, the concentrations of key elements (PG, anti-MPT64, APP2), the RCA time, and the pH of working solution. APP2 is chosen to be used in the next experiments. The optimal concentrations of PG, anti-MPT64 and APP2 are 15 μg·mL^{-1}, 20 μg·mL^{-1} and 200 nmol·L^{-1}, respectively. The

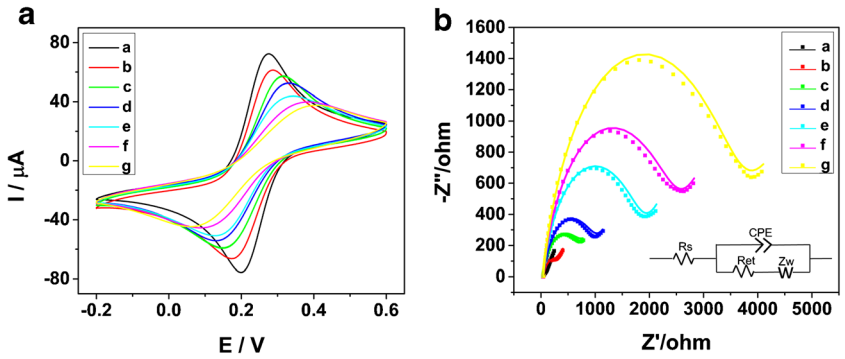

Fig. 2 Electrochemical characterization of the modified electrode. **a** Cyclic voltammetry results and **b** Nyquist plots (including fitting curves) obtained from different electrodes: (a) bare gold electrode, (b) PG/gold electrode, (c) Ab/PG/gold electrode, (d) BSA/Ab/PG/gold electrode, (e) MPT64/BSA/Ab/PG/gold electrode, (f) APP/MPT64/BSA/Ab/PG/gold electrode, (g) RCPs/APP/MPT64/BSA/Ab/PG/gold electrode. These experiments were performed in PB working solution (10 mmol·L^{-1}, pH 7.4) containing 5 mmol·L^{-1} $[Fe(CN)_6]^{3-/4-}$ and 0.1 mol·L^{-1} KCl (scan rate of CV: 0.1 V/S)

optimal reaction time of RCA is 60 min. The suitable working solution pH is 4.0. (Fig. S6).

Analytical property of the biosensor

Linearity range and limit of detection

Under the optimized experimental conditions, different concentrations of MPT64 were detected by the biosensor. As shown in Fig. 3a, the DPV current signal is increased with the increasing concentration of MPT64. Moreover, the current signal intensity shows a good linear relationship with the logarithm of MPT64 concentration ranging from 5.0 fg·mL^{-1} to 1.0×10^6 fg·mL^{-1}. The calibration plot is depicted in Fig. 3b. The linear regression equation is I (μA) = 2.713logc + 10.873 with a linear correlation coefficient (R^2) of 0.9962. The detection limit (LOD) was estimated to be 0.34 fg·mL^{-1} (signal to noise ratio: 3, n = 10) which was calculated by the following equation: LOD = 3SD/k (*SD* represents the standard deviation of the blank, k represents the slope of the linear regression equation) [27]. Compared with other methods of *MTb* detection, the biosensor displays a good performance in analytical range and detection limit (Table 1) which indicate that it is a promising strategy for *MTb* detection.

Specificity

The specificity of the biosensor was assessed by detecting several interfering proteins such as BSA, *MTb* secretory protein Ag85B (Ag85B), procalcitonin (PCT), glucose-regulated protein 78 (GRP78) and inhibitor of differentiation (ID). Under the same experimental conditions, there are negligible current changes among those interfering proteins when compared with blank. However, a strong current response is observed with the presence of MPT64 (Fig. 3c). These results indicate that the biosensor has a high specificity.

Repeatability

The repeatability of the biosensor is studied by measuring different concentrations of MPT64 (1.0×10^2, 1.0×10^4, 1.0×10^6 fg·mL^{-1}) for 10 times (Fig. S7). The relative standard deviation (RSD) is used to assess the repeatability. They were 3.66%, 3.76%, and 2.60%, respectively (n = 10).

Stability

The stability of the biosensor was studied by measuring MPT64 at different time points during storage. As shown in

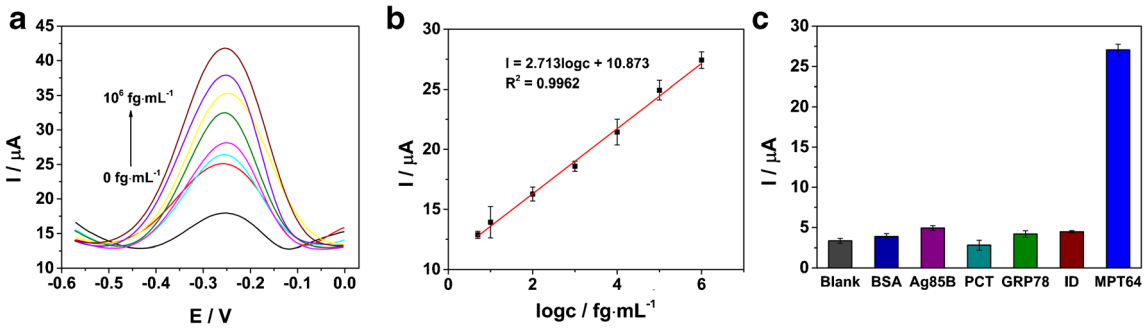

Fig. 3 Analytical property of the electrochemical biosensor. **a** DPV curves of different concentrations of MPT64 (0, 5, 10, 10^2, 10^3, 10^4, 10^5, 10^6 fg·mL^{-1}). **b** The calibration plot showing the relationship between the DPV current signal obtained at −0.25 V and the logarithm of MPT64 concentration. **c** Specificity of the biosensor toward different analytes with the same concentration of 1 ng·mL^{-1} (Error bars = SD, n = 5)

Table 1 Performance comparison for *MTb* detection

Detection method	*MTb* target	Linearity range	LOD	References
Voltammetry	MPT64	1.0 fg·mL^{-1}–1.0 × 10^5 fg·mL^{-1}	0.9 fg·mL^{-1}	[10]
Voltammetry	*MTb* DNA sequence	0.1 pM–10 nM	50 fM	[20]
Impedance	16 kD heat shock protein	100 fM–1 nM	100 fM	[28]
ELISA	MPT64	2.1 ng·mL^{-1}–250 ng·mL^{-1}	2.1 ng·mL^{-1}	[29]
Voltammetry	MPT64	1.0 × 10^3 fg·mL^{-1}–1.0 × 10^7 fg·mL^{-1}	0.3 fg·mL^{-1}	[30]
Voltammetry	MPT64	20 fg·mL^{-1}–1.0 × 10^6 fg·mL^{-1}	20 fg·mL^{-1}	[31]
Voltammetry	MPT64	5.0 fg·mL^{-1}–1.0 × 10^6 fg·mL^{-1}	0.34 fg·mL^{-1}	This work

Table S3, the biosensor shows good stability within 15 days' storage at 4 °C by immersed in PB. Compared with initial current signal of the biosensor, the current signal retains 97.31%, 95.21%, and 90.23%, respectively, by measuring at 5, 10, and 15 days' storage.

Clinical application

Recovery test

In order to evaluate the feasibility of the biosensor for clinical application, recovery tests were performed by the standard addition method in healthy human serum samples. The serum samples were spiked with MPT64 at concentrations of 10.0 fg·mL^{-1}, 1.0 × 10^3 fg·mL^{-1}and 1.0 × 10^5 fg·mL^{-1}, respectively. Then, these serum samples were quantified by the biosensor, and the corresponding results were listed in Table S4. The recovery values range from 97.97 to 106.50% and the relative standard deviation range from 2.50 to 3.13% ($n = 5$). These results indicate that the biosensor had great potential in clinical application for the detection of MPT64 in serum samples.

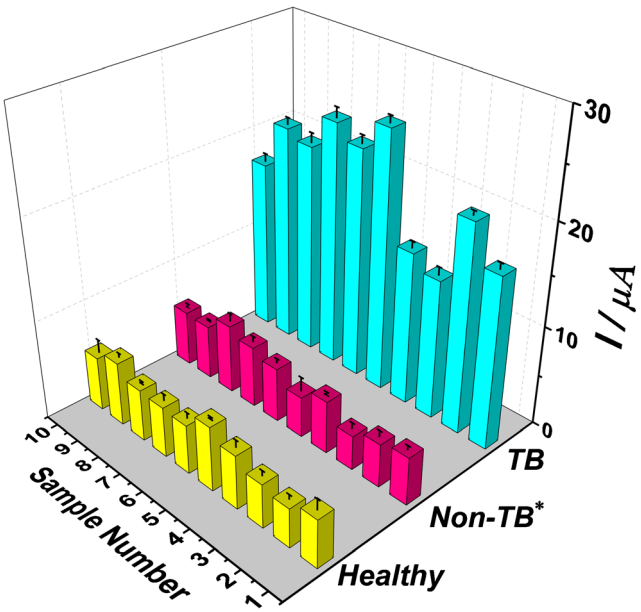

Fig. 4 Detection of MPT64 in clinical serum samples (Error bars = SD, $n = 5$). * Non-TB represents the serum samples collected from the patients with other bacterial pulmonary infections

Detection of MPT64 in clinical serum samples

To further prove the feasibility of the biosensor, we tried to detect MPT64 in thirty clinical serum samples. These serum samples were collected from The First Affiliated Hospital of Chongqing Medical University, including the TB group, healthy group, and non-TB group. The non-TB group serum samples were provided by the patients with other bacterial pulmonary infections such as *Pseudomonas aeruginosa, Klebsiella pneumoniae,* and *Haemophilus influenzae*. Each group has ten serum samples. As shown in Fig. 4, negligible current signals are observed when the biosensor is applied to detect the serum samples of healthy group $\left(\overline{x} = 5.22 \pm 0.79\ \mu A, n_{sample} = 10\right)$ and non-TB group $\left(\overline{x} = 5.31 \pm 1.02\ \mu A, n_{sample} = 10\right)$, respectively. However, when the biosensor is applied to detect the serum samples of TB group, significantly high current signals $\left(\overline{x} = 19.96 \pm 3.92\ \mu A, n_{sample} = 10\right)$ are obtained, indicating the existence of MPT64 in these TB group samples. These results suggest that the electrochemical biosensor can effectively identify *MTb* infection by detecting *MTb* secretory protein MPT64.

Conclusion

In summary, a novel electrochemical biosensor was constructed for ultrasensitive and rapid detection of MPT64 with the synergetic signal amplification strategy of RCA and GO@Fe_3O_4@Pt nanocomposite. GO with its large surface area was used as a carrier to anchor Fe_3O_4 and Pt nanoparticles. GO@Fe_3O_4@Pt nanocomposite was a well signal reporter for its excellent catalytic activity and recyclability. Based on this, the biosensor had a wide linearity range and low detection limit of 0.34 fg·mL^{-1}. Moreover, the detection process was completed within 4 h, which might contribute to rapid diagnosis of TB. More importantly, this biosensor was successfully applied to detect MPT64 in clinical serum

samples to discriminate *MTb* infection. This electrochemical biosensor has been shown to have broad application potential for early and rapid diagnosis of TB. However, this method also has some limitations. The number of reuses of GO@Fe_3O_4@Pt nanocomposite still needs to be improved. The synthesis process of nanomaterial is relatively sophisticated. And present method is not assembled to a POCT device for clinical direct use. In future research, we will attempt to assemble this electrochemical biosensor into electrochemical biochip sensor for simultaneous detection of multi-markers.

Acknowledgements This research work was financially supported by the National Natural Science Foundation of China (No. 81672112).

Compliance with ethical standards The author(s) declare that they have no competing interests.

References

1. Turbawaty DK, Sugianli AK, Soeroto AY, Setiabudiawan B, Parwati I (2017) Comparison of the performance of urinary Mycobacterium tuberculosis antigens cocktail (ESAT6, CFP10, and MPT64) with culture and microscopy in pulmonary tuberculosis patients. Int J Microbiol 2017:1–5 https://doi.org/10.1155/2017/3259329
2. World Health Organization (2017) Global tuberculosis report 2017. Available from: http://wwwwhoint/tb/publications/global_report/en/ Accessed 10 March 2018
3. Caceres N, Vilaplana C, Prats C, Marzo E, Llopis I, Valls J, Lopez D, Cardona PJ (2013) Evolution and role of corded cell aggregation in Mycobacterium tuberculosis cultures. Tuberculosis (Edinb) 93(6):690–698 https://doi.org/10.1016/j.tube.2013.08.003
4. Steingart KR, Ng V, Henry M, Hopewell PC, Ramsay A, Cunningham J, Urbanczik R, Perkins MD, Aziz MA, Pai M (2006) Sputum processing methods to improve the sensitivity of smear microscopy for tuberculosis: a systematic review. Lancet Infect Dis 6(10):664–674 https://doi.org/10.1016/s1473-3099(06)70602-8
5. Wang X, Xie F, Zheng Q, Qi X, Li M, Zhou X, Zheng Z (2017) Fluorescent quantitative PCR detection of Mycobacterium tuberculosis in tissue sections from granulomatous lesions retrieved using EDTA. J Clin Pathol 70(5):390–394 https://doi.org/10.1136/jclinpath-2016-203738
6. Kim EJ, Kim EB, Lee SW, Cheon SA, Kim HJ, Lee J, Lee MK, Ko S, Park TJ (2017) An easy and sensitive sandwich assay for detection of Mycobacterium tuberculosis Ag85B antigen using quantum dots and gold nanorods. Biosens Bioelectron 87:150–156 https://doi.org/10.1016/j.bios.2016.08.034
7. Yin X, Zheng L, Lin L, Hu Y, Zheng F, Hu Y, Wang Q (2013) Commercial MPT64-based tests for rapid identification of Mycobacterium tuberculosis complex: a meta-analysis. J Inf Secur 67(5):369–377 https://doi.org/10.1016/j.jinf.2013.06.009
8. Purohit MR, Sviland L, Wiker H, Mustafa T (2017) Rapid and specific diagnosis of extrapulmonary tuberculosis by immunostaining of tissues and aspirates with anti-MPT64. Appl Immunohistochem Mol Morphol 25(4):282–288 https://doi.org/10.1097/PAI.0000000000000300
9. Islamov M, Sypabekova M, Kanayeva D, Rojas-Solorzano L (2017) CFD modeling of chamber filling in a micro-biosensor for protein detection. Biosensors (Basel) 7(4) https://doi.org/10.3390/bios7040045
10. Thakur H, Kaur N, Sabherwal P, Sareen D, Prabhakar N (2017) Aptamer based voltammetric biosensor for the detection of Mycobacterium tuberculosis antigen MPT64. Microchim Acta 184(7):1915–1922 https://doi.org/10.1007/s00604-017-2174-7
11. Parvin N, Jin Q, Wei Y, Yu R, Zheng B, Huang L, Zhang Y, Wang L, Zhang H, Gao M, Zhao H, Hu W, Li Y, Wang D (2017) Few-layer graphdiyne nanosheets applied for multiplexed real-time DNA detection. Adv Mater 29(18):1606755 https://doi.org/10.1002/adma.201606755
12. Cai J, Huang J, Ge M, Iocozzia J, Lin Z, Zhang KQ, Lai Y (2017) Immobilization of Pt nanoparticles via rapid and reusable electropolymerization of dopamine on TiO2 nanotube arrays for reversible SERS substrates and nonenzymatic glucose sensors. Small 13(19) https://doi.org/10.1002/smll.201604240
13. Ali MM, Li F, Zhang Z, Zhang K, Kang DK, Ankrum JA, Le XC, Zhao W (2014) Rolling circle amplification: a versatile tool for chemical biology, materials science and medicine. Chem Soc Rev 43(10):3324–3341 https://doi.org/10.1039/c3cs60439j
14. Zhang S, Wang K, Li KB, Shi W, Jia WP, Chen X, Sun T, Han DM (2017) A DNA-stabilized silver nanoclusters/graphene oxide-based platform for the sensitive detection of DNA through hybridization chain reaction. Biosens Bioelectron 91:374–379 https://doi.org/10.1016/j.bios.2016.12.060
15. Rafati A, Gill P (2014) Microfluidic method for rapid turbidimetric detection of the DNA of Mycobacterium tuberculosis using loop-mediated isothermal amplification in capillary tubes. Microchim Acta 182(3–4):523–530 https://doi.org/10.1007/s00604-014-1354-y
16. Takenaka M, Amino T, Miyachi Y, Ogino C, Kondo A (2017) Screening and evaluation of aptamers against somatostatin, and sandwich-like monitoring of somatostatin based on atomic force microscopy. Sensors Actuators B Chem 252:813–821 https://doi.org/10.1016/j.snb.2017.06.019
17. Zhou D, Xie G, Cao X, Chen X, Zhang X, Chen H (2016) Colorimetric determination of staphylococcal enterotoxin B via DNAzyme-guided growth of gold nanoparticles. Microchim Acta 183(10):2753–2760 https://doi.org/10.1007/s00604-016-1919-z
18. Casalini S, Dumitru AC, Leonardi F, Bortolotti CA, Herruzo ET, Campana A, de Oliveira RF, Cramer T, Garcia R, Biscarini F (2015) Multiscale sensing of antibody-antigen interactions by organic transistors and single-molecule force spectroscopy. ACS Nano 9(5):5051–5062 https://doi.org/10.1021/acsnano.5b00136
19. Lee H, Choi TK, Lee YB, Cho HR, Ghaffari R, Wang L, Choi HJ, Chung TD, Lu N, Hyeon T, Choi SH, Kim DH (2016) A graphene-based electrochemical device with thermoresponsive microneedles for diabetes monitoring and therapy. Nat Nanotechnol 11(6):566–572 https://doi.org/10.1038/nnano.2016.38
20. Chen Y, Li Y, Yang Y, Wu F, Cao J, Bai L (2017) A polyaniline-reduced graphene oxide nanocomposite as a redox nanoprobe in a voltammetric DNA biosensor for Mycobacterium tuberculosis. Microchim Acta 184(6):1801–1808 https://doi.org/10.1007/s00604-017-2184-5
21. Li Y, Pu Q, Li J, Zhou L, Tao Y, Li Y, Yu W, Xie G (2017) An "off-on" fluorescent switch assay for microRNA using nonenzymatic ligation-rolling circle amplification. Microchim Acta 184(11):4323–4330 https://doi.org/10.1007/s00604-017-2475-x
22. Iranmanesh M, Hulliger J (2017) Magnetic separation: its application in mining, waste purification, medicine, biochemistry and chemistry. Chem Soc Rev 46(19):5925–5934 https://doi.org/10.1039/c7cs00230k
23. Gao L, Zhuang J, Nie L, Zhang J, Zhang Y, Gu N, Wang T, Feng J, Yang D, Perrett S, Yan X (2007) Intrinsic peroxidase-like activity of ferromagnetic nanoparticles. Nat Nanotechnol 2(9):577–583 https://doi.org/10.1038/nnano.2007.260
24. Dendooven J, Ramachandran RK, Solano E, Kurttepeli M, Geerts L, Heremans G, Ronge J, Minjauw MM, Dobbelaere T, Devloo-

Casier K, Martens JA, Vantomme A, Bals S, Portale G, Coati A, Detavernier C (2017) Independent tuning of size and coverage of supported Pt nanoparticles using atomic layer deposition. Nat Commun 8(1):1074 https://doi.org/10.1038/s41467-017-01140-z

25. Roh YH, Deng JZ, Dreaden EC, Park JH, Yun DS, Shopsowitz KE, Hammond PT (2016) A multi-RNAi microsponge platform for simultaneous controlled delivery of multiple small interfering RNAs. Angew Chem Int Ed Eng 55(10):3347–3351 https://doi.org/10.1002/anie.201508978
26. Yang Z, Zhao Y-P (2007) Adsorption of his-tagged peptide to Ni, cu and au (100) surfaces: molecular dynamics simulation. Engineering Analysis with Boundary Elements 31(5):402–409 https://doi.org/10.1016/j.enganabound.2006.07.012
27. Feng C, Bo B, Mao X, Shi H, Zhu X, Li G (2017) From interface to solution: integrating immunoassay with netlike rolling circle amplification for ultrasensitive detection of tumor biomarker. Theranostics 7(1):31–39 https://doi.org/10.7150/thno.16671
28. Gopinath SCB, Perumal V, Kumaresan R, Lakshmipriya T, Rajintraprasad H, Rao BS, Arshad MKM, Chen Y, Kotani N, Hashim U (2016) Nanogapped impedimetric immunosensor for the detection of 16 kDa heat shock protein against Mycobacterium tuberculosis. Microchim Acta 183(10):2697–2703 https://doi.org/10.1007/s00604-016-1911-7
29. Ji M, Cho B, Cho YS, Park SY, Cho SN, Jeon BY, Yoon BS (2014) Development of a quantitative sandwich enzyme-linked immunosorbent assay for detecting the MPT64 antigen of Mycobacterium tuberculosis. Yonsei Med J 55(3):746–752 https://doi.org/10.3349/ymj.2014.55.3.746
30. Thakur H, Kaur N, Sareen D, Prabhakar N (2017) Electrochemical determination of M. Tuberculosis antigen based on poly(3,4-ethylenedioxythiophene) and functionalized carbon nanotubes hybrid platform. Talanta 171:115–123 https://doi.org/10.1016/j.talanta.2017.04.063
31. Bai L, Chen Y, Bai Y, Chen Y, Zhou J, Huang A (2017) Fullerene-doped polyaniline as new redox nanoprobe and catalyst in electrochemical aptasensor for ultrasensitive detection of Mycobacterium tuberculosis MPT64 antigen in human serum. Biomaterials 133:11–19 https://doi.org/10.1016/j.biomaterials.2017.04.010